A COMPARATIVE STUDY IN PHOTOCATALYTIC DEGRADATION OF COOMASSIE BRILLIANT BLUE G DYE BY USING NICKEL CALCIATE NANOPARTICLES

Santhosh A. M.
Research Scholar, Department of P.G studies and Research in Environmental Science, Kuvempu University, JnanaSahyadri, Shankaraghatta, Shivamogga, Karnataka, India.
Yogendra K†
Assistant Professor, Department of P.G studies and Research in Environmental Science, Kuvempu University, JnanaSahyadri, Shankaraghatta, Shivamogga, Karnataka, India.
Mahadevan K.M.
Professor, Department of P.G studies and Research in Chemistry, Kadur P.G Center, Kuvempu University, Kadur, Karnataka, India.
Mallikarjuna I.H.
Assistant Professor, Department of Chemistry, Government Science College, Hassan, Karnataka, India.
Madhusudhana N.
Post Doctoral Fellow, Department of P.G studies and Research in Environmental Science, Kuvempu University, JnanaSahyadri, Shankaraghatta, Shivamogga, Karnataka, India

ABSTRACT-The photodegradation efficiency of two synthesized Nickel Calciate nanoparticles ($NiCaO_2$-I and $NiCaO_2$-II) against Coomassie Brilliant Blue G (CBBG) dye in aqueous solution was investigated. The Nickel Calciate nanoparticles were synthesized by solution combustion method using two different fuels urea and acetamide. The synthesized nanoparticles were characterized by SEM, XRD, EDX and the band gap was determined by using UV-absorption spectroscopy. All the experiments were conducted in presence of natural sun light. Degradation efficiency was studied by varying different parameters such as catalyst concentration, solution pH, dye concentration and in different conditions with respect to UV and dark conditions.

Keywords: Photodegradation, Nanoparticles, $NiCaO_2$, Coomassie Brilliant Blue G (CBBG).

1. INTRODUCTION

Dyes are widely used in the textile, leather, paper, printing inks, plastics, cosmetics, paints, pharmaceutical, and food industries [1]. The total world colorant production in 2008 was recorded to be about 1.5 million tons. It is estimated that 15% of these dyes is lost in the synthesis, processing of colorants, dyeing, printing and finishing [2]. The usage of these industrial dyes is maximum hence we find the contaminated river water streams and sewage treatment plants in urban areas [3]. Even though the concentration of dye in wastewaters is very low compared to other chemicals, it's strong affinity towards water makes it visible even at very low concentrations, thus causing serious aesthetic and pollution problems in wastewater disposal [4, 5] and also these dyes can harm the environment especially the aquatic ecosystem. Coloured effluents released by different industries may be mutagenic, carcinogenic and toxic. Synthetic dyes are usually treated by physical or chemical methods [6].

A non-azo dye, CBBG, have been used for the purpose of acid wool dye and known to be popular reagent for protein chemists. This is widely used for staining proteins in electrophoresis techniques, as well as for measuring protein [7]. In the earlier studies other researcher have investigated the degradation of CBBG by different nanoparticles like Ce and Nd-doped Bi_2O_3, [8] La and Mo-doped TiO_2, [9] Cerium-Iron Oxide, [10] palladium nanoparticles [11] and also Jadhav et al., decolorize the CBBG dye by microbial consortium of Galactomyces geotrichum and *Bacillus sp*. [12] Arunachalam *et al., has* degraded the CBBR by green synthesized silver nanoparticles [13].

In recent years, much attention is given to photocatalytic decolourization of Industrial dyes and coloured effluents in presence natural sunlight. Since it's a cost-effective alternate for the purification of dye containing wastewater [14], photocatalysis, has become one of the advanced processes in pollution prevention. In this method mineralizes the dye compounds [2] and also light energy observed by the semiconductor material, which is equal to or more than to its band gap, thereby creates electrons holes for the release of free radicals in the system to oxidize the substrate and the resultant free-radicals are very efficient oxidizers of organic compounds [15, 16, 3]. The frequent use of photocatalytic oxidation technology for the complete removal of dyes in wastewater by utilizing sunlight and UV irradiation as energy sources [17]. Keeping in view of importance of photocatalysis, and in continuation of our study in decolourization of dyes, [3, 14, 15, 18-22) we aimed at the synthesis of Nickel Calciate ($NiCaO_2$) nanoparticles for decolourization of CBBG dye, which is being used extensively in textile industries.

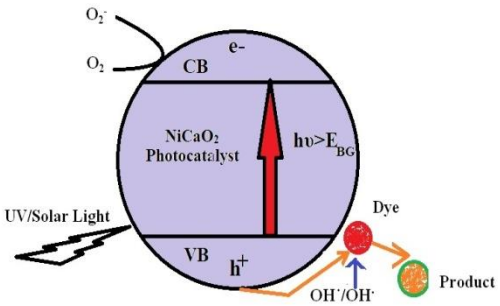

Figure 1: Mechanism of photocatalytic Degradation

2. EXPERIMENTAL DETAILS

The commercially available water soluble dyes CBBG (λ_{max} 582nm) were obtained from Sisco Research Laboratory Pvt. Ltd. Maharastra (Figure 2). The chemicals like Nickel Nitrate ($Ni(NO_3)_2.6H_2O$) (99% A. R.), are obtained from Sisco Research Laboratory Pvt. Ltd. Maharastra Calcium Nitrate ($Ca(NO_3)_2.4H_2O$) (99%, A. R.), Urea (NH_2CONH_2) (99.5%), Acetamide (CH_3CONH_2) (99%, A.R.), were obtained from Hi-Media Chemicals, Mumbai. The visible spectrophotometer (Elico, SL 177) has been used for recording absorbance at λ_{max}. Later the absorbance was recorded in visible spectrophotometer (Elico, SL 177).

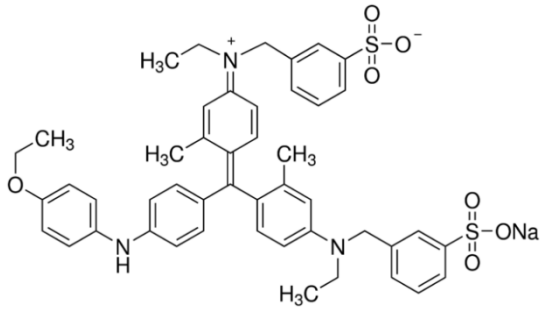

Figure 2: Chemical Structure of Coomassie Brilliant Blue G

2.1. SYNTHESIS OF NANOPARTICLES

The $NiCaO_2$ nanoparticles were synthesized by solution combustion method, using oxidizers (metal nitrates) and fuels (urea, acetamide). It involves a self-sustained reaction in homogeneous solution of different oxidizers and fuels. In the first stage $NiCaO_2$-I was prepared by using the fuel Urea and $NiCaO_2$-II by using acetamide. Here urea and acetamide are used as fules for the synthesis process. Both urea and Acetamide will provide the required amount of Hydrogen and Oxygen to the combustion process, which intern help the reaction through converting the nitrogen into ammonia and converting the metal nitrates into oxides, which helps to build the different morphology for different nanoparticles. Hence both the fuels play a vital role in the combustion synthesis process. Stoichiometric amounts of Nickel Nitrate, Calcium Nitrate, and fuels Urea and Acetamide were calculated using the total oxidizing and reducing valences of the compounds which serve as numerical coefficients for Stoichiometric balance. For $NiCaO_2$-I the chemicals of Nickel Nitrate (5.48g), Calcium Nitrate (7.08g), and were dissolved in minimum quantity of water along with Urea (6.05g) and similarly for $NiCaO_2$-II synthesis, Nickel Nitrate (20.9 g), Calcium Nitrate (25.98 g), along with the fuel Acetamide (11.81 g) in a silica crucible (with volume of 100 cm^3). The crucible was introduced into the muffle furnace which was preheated to 600° C. The solution boils and undergoes dehydration followed by decomposition along with the release of certain amounts of gases it froths and swells forming foam which ruptures with a flame and glows to incandescence. The obtained nano particle was crushed in a mortar to make it amorphous and used for the photocatalytic degradation study of CBBG (λ_{max} 582nm). According to the propellant chemistry, the following reaction takes place during combustion.

$$3Ni(NO_3)_2+3Ca(NO_3)_2+10NH_2CONH_2 \rightarrow 3NiCaO_2+10CO_2+20H_2O+16N_2 \quad (1)$$

$$11Ni(NO_3)_2+11Ca(NO_3)_2+20CH_3CONH_2 \rightarrow 11NiCaO_2+50CO_2+40H_2O+32N_2 \quad (2)$$

2.2. POINT OF ZERO CHARGE

Point of zero charge or isoelectric point is the pH of the solution at which the total charge on the surface of the nanoparticles becomes zero (neutral). The point of zero charge of $NiCaO_2$ were measured by pH drift method, 50ml of NaCl 0.01M was taken in six separate beakers and bubbled it with Nitrogen gas to expel the dissolved CO_2 for few minutes at room temperature till it get a stable pH reading. The pH of the solution in each beaker was adjusted between 2 to 12 by adding 0.1N HCl and 0.1N NaOH after which 50mg of $NiCaO_2$ nanoparticles were added. This system was kept at room temperature until concurrent pH measured; this was kept for 92hrs for the stabilization of pH. The graph was plotted against final pH v/s initial pH, the point which this curve crosses the initial pH=final pH straight line is the point of zero charge.

2.3. CHARACTERIZATION OF NANOPARTICLES

Powder X-ray diffraction (XRD) was performed powder X-ray diffraction (Rigaku diffractrometer) using Cu-Kα radiation (1.5406 Å) in a θ-2θ configuration. Specific surface areas (SSA) of the photocatalysts were estimated at 77 K by Brunauer–Emmett–Teller (BET) nitrogen adsorption–desorption (NOVA-1000 version 3.70 Instrument). Scanning electron microscope

(SEM) image was taken with a JEOL (JSM-840A). The UV-visible spectra of the photocatalysts were carried out using a UV-visible spectrophotometer in the λ range from 200 to 1200 nm. The confirmatory presence of elements was carried out using Energy Dispersive X-ray (EDX) spectrometer.

2.4. EXPERIMENTAL PROCEDURE

The photocatalytic experiments were carried out under direct sunlight. The known concentration of dye solutions were prepared by dissolving 0.02g of CBBG in 1000ml double distilled water and investigated for its decolourization in the presence of Nickel Calciate nanoparticle at different catalyst dosages and pH levels. Initially, 100ml of 20ppm of dye samples were tested with different catalyst dosage (from 0. 1g to 1g), by varying pH (from 2pH to 11pH), dye concentration (20ppm to 50ppm and different conditions with respect to U.V and dark. Except U.V and dark conditions all experiments carried out in the presence of direct sunlight. The whole experimental set-up was placed in sunlight between 11 a.m. and 2 p.m. and the average intensity of sunlight during this period is 792×100 lux unit using lux meter. After the photocatalytic decolourization, the extent of decolourization was estimated by recording absorbance of the dye solution using spectrophotometer (Elico, SL 177) in order to get the optimum catalyst dose. The experiments were repeated at different pH levels (from 2 to 11) for the 100ml of same standard dye solutions with the optimum catalyst dose. Initial dye concentration and different conditions experiments were repeated at different concentration and different conditions with respect to U.V. and dark conditions for the 100ml of same standard dye solution with optimum catalyst and pH. The percentage was calculated by equation,

$$D=C_o\text{-}C_t/C_o\times \qquad (3)$$

Where, $\mathbf{C_0}$ is the initial absorbance of the dye solution $\mathbf{C_t}$ is absorbance at time interval‘t’ i.e., after 120 minutes.

3. RESULT AND DISCUSSION

3.1. BET SURFACE ANALYSIS

The results of the Brunauer–Emmett–Teller surface area measurements of the as-prepared $NiCaO_2$-I and $NiCaO_2$-II were 2.4416 m^2/g and 2.3778 m^2/g respectively. BET surface area analysis, the specific surface area and pore volumes obtained for the nanoparticles are reported in table 1. This value is analogues to the other nanoparticles [23-25]. The obtained surface area for $NiCaO_2$ nanoparticles is suitable for the photocatalytic activity [26].

Table 1: Surface properties of the nanoparticles

Catalyst	Surface area	Pore volume	Average pore diameter
$NiCaO_2$ (urea)	2.4416 m^2/g	0.01013 cc/g	165.87Å
$NiCaO_2$ (acetamide)	2.3778 m^2/g	0.00265 cc/g	44.578Å

3.2. NATURE OF ZERO POINT CHARGE

In order to understand the behaviour of adsorption or photocatalysts with respect to pH, it is important to determine the isoelectric point or point zero charge of the nanoparticles. For the determination of PZC of $NiCaO_2$-I and $NiCaO_2$-II nanoparticles, the graph of initial pH against final pH was plotted and the values of $pH_{(pzc)}$ were found to be 11.5 and 11.7 respectively. (Figure 3a) Below this $pH_{(pzc)}$ the surface is acidic in nature, positively charged and above this surface is basic in nature and negatively charged. The pH of CBBG is below the $pH_{(pzc)}$, which favours the adsorption of anionic CBBG and thus the suitable for photocatalysis [27].

3.3. SCANNING ELECTRON MICROSCOPY

The powdered sample was examined by SEM technique which shows that, the structure of the synthesized $NiCaO_2$-I and $NiCaO_2$-II nanoparticles. An image obtained by SEM analysis reveals the agglomeration and arrange in the clumpy form [28] for both synthesized $NiCaO_2$ nanoparticles presented in Figure 3b and 3c.

3.4. X-RAY DIFFRACTION (XRD)

The XRD patterns of $NiCaO_2$-I and $NiCaO_2$-II nanoparticles reveal that, the presence of Rhombo Hedral structure and the 2θ peaks were observed which related to Nickel oxide, (36.67°, 42.72°, 54.00°, 62.26°) (JCPDS card No.01-089-3080) Caliate (28.97°, 39.02°, 46.78°) (JCPDS card No.00-003-0569) for $NiCaO_2$-I and for $NiCaO_2$-II the peaks were related to Nickel oxide, (37.29°, 43.30°, 62.87°, 75.40°, 79.33°) (JCPDS card No.01-089-3080) Caliate (23.13°, 29.48°, 39.48, 48.59°, 57.48°) (JCPDS card No.00-024-0027) and the XRD was performed by powder X-ray diffraction (Rigaku diffractometer) using Cu-Kα radiation (1.5406 Å) in a θ-2θ configuration. The pattern obtained from the XRD analysis of the prepared $NiCaO_2$-I and $NiCaO_2$-II nanoparticles were presented in Figure 3d and 3e.

According to the Debye Scherrer’s formula: $D=K\lambda/\beta \cos\theta$ (4)

K = 0.90 the Scherrer’s constant (dependent on crystallite shape)

λ = X-ray wavelength

β = the peak full width at half-maximum (FWHM)

θ = the Bragg diffraction angle

In the present work, the powdered sample of newly synthesized $NiCaO_2$-I and $NiCaO_2$-II nanoparticles were examined by XRD studies and found that $NiCaO_2$-I nanoparticle size varies from 8 nm to 18 nm and henceforth the average crystallite size was found to be 14 nm. Whereas $NiCaO_2$-II nanoparticles found to be varied from 10 nm to 24 nm and its average size was achieved on 19 nm respectively

3.5. UV ABSORPTION SPECTROSCOPY

The optical absorption is an important tool to obtain optical energy band gap of crystalline and amorphous materials. The fundamental absorption corresponds to the electron excitation from the valence band to the conduction band can be used to determine the nature and value of the optical band gap. The absorption spectrum reveals that the $NaCaO_2$-I and $NaCaO_2$-II nanoparticles (Figure 3f and 3g) absorption in the visible light region with a wavelength above 400 nm. The optical energy band gap Eg is calculated from the relation: $(\alpha h\upsilon)=B(h\upsilon-Eg)^n$ Where, 'hυ' is the photon energy, 'B' is the constant and 'n' is the power factor and that takes 1/2, 2, 3/2 and 3 allowed direct, allowed indirect, forbidden direct and forbidden indirect transitions respectively. The optical band gap of the the $NaCaO_2$-I and $NaCaO_2$-II nanoparticle found to be 3.05eV and 2.86eV respectively.

3.6. ENERGY DISPERSIVE X-RAY (EDX)

Energy Dispersive X-ray (EDX) spectrometer analysis is confirmatory presence of elemental Nickel, calcium, carbon and Oxygen signals of the Nickel Calciate nanoparticles. The vertical axis displays the number of x-ray counts although the horizontal axis displays energy in KeV (Figure 3h and 3i). The weight and atomic percentage of carbon, Oxygen, calcium, and Nickel was found to be 7.79, 51.80, 25.74, 14.67 and 13.57, 67.76, 13.44, 5.23 for $NiCaO_2$ - I and $NiCaO_2$ - II found to be 20.57, 46.88, 17.85, 14.69 and 32.08, 54.88, 8.344.69 these corresponds, the spectrum without impurities peaks [29].

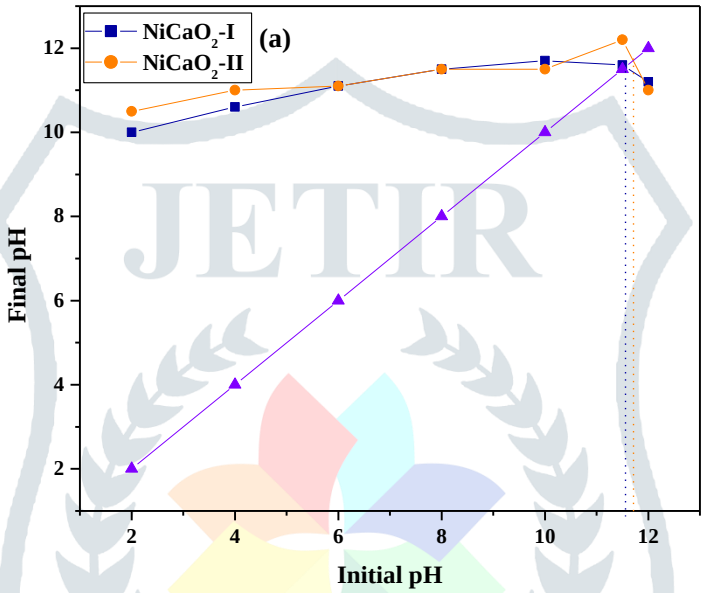

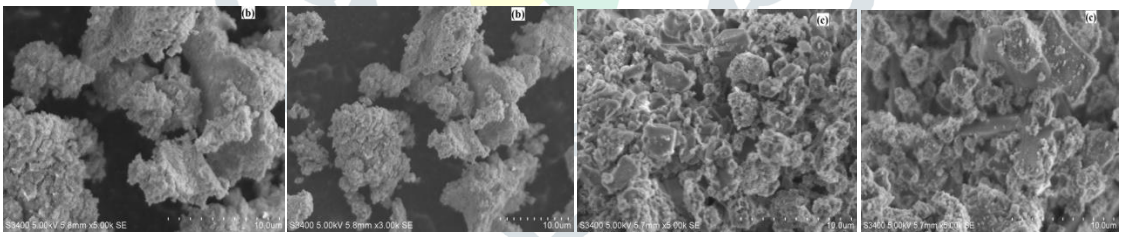

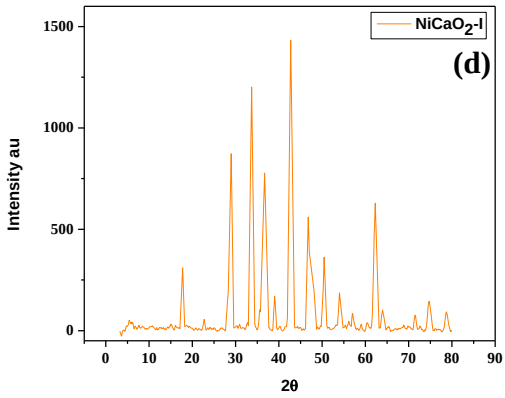

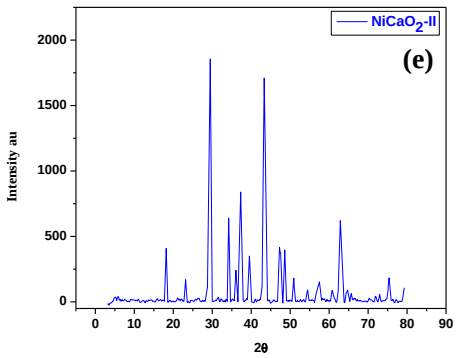

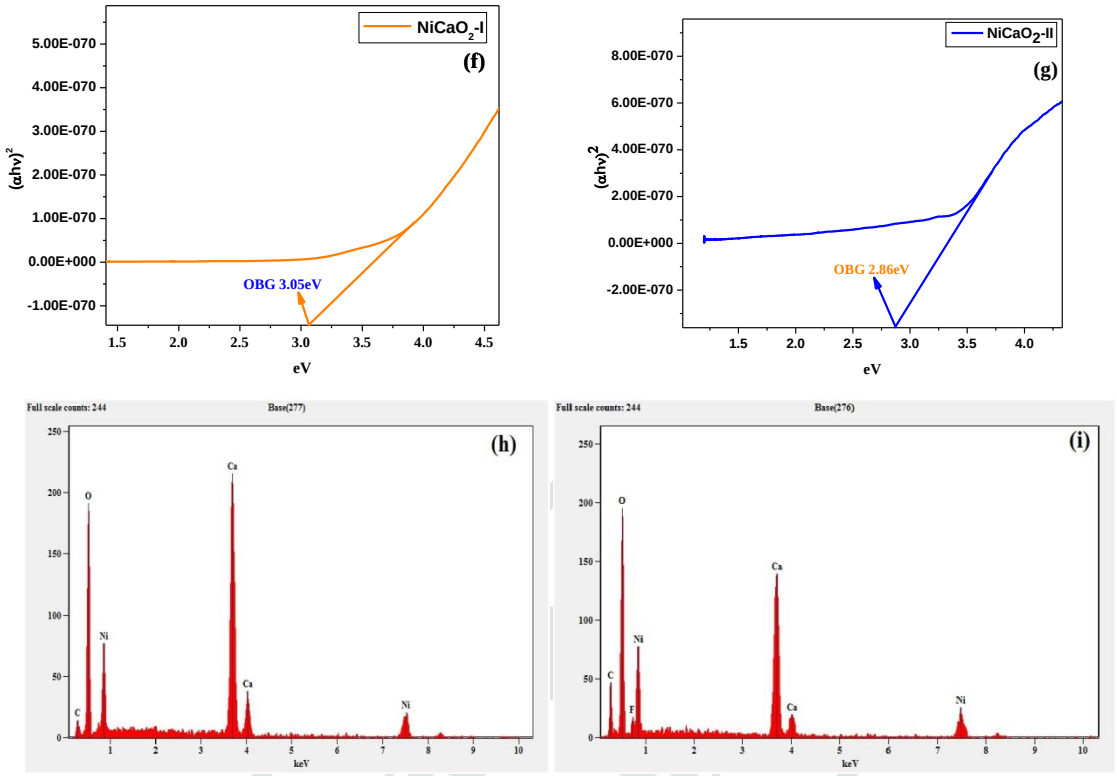

Figure 3: (a) point of Zero Charge of $NiCaO_2$ nanoparticles, Scanning Electron Micrographs (b) $NiCaO_2$ – I (c) $NiCaO_2$ – II, XRD (d) $NiCaO_2$-I (e) $NiCaO_2$ –II, UV-absorption spectra (f) $NiCaO_2$ – I (g) $NiCaO_2$ – II, Energy Dispersive X-ray (h) $NiCaO_2$ – I (i) $NiCaO_2$ – II.

3.7. EFFECT OF CATALYST CONCENTRATION

The catalyst concentration studies for the degradation of CBBG dye was investigated, the amount of catalyst varies from 0.1g to 1g/100ml. The percentage of degradation of dye has shown appreciable results. Where, $NiCaO_2$-I (Figure 4a) (Figure 5a) showed maximum of 97.35 % at 0.3g/100ml, $NiCaO_2$-II (Figure 4b) (Figure 5b) showed 95.03% at 0.4g/100ml in 120 minutes. The $NiCaO_2$-I with the nanoparticle size of 14nm has shown maximum degradation when compared to the other synthesized nanoparticle $NiCaO_2$-II of size 19nm. Thus we can say, the degradation is also depend on the size of the nanoparticles, the size of the $NiCaO_2$-I (14nm) nanoparticle is small when compared to the $NiCaO_2$-II (19nm).

Figure 4a and b illustrated that, the concentration of the nanoparticles increases the degradation efficiency of CBBG dye, also it is described by increase in number of active area of the catalyst and availability of the irradiation has led to increased screening effect and scattering of light. On further increasing the catalyst beyond optimum dose it decreases the photocatalytic activity. This is due to higher the catalyst loading, the overlapping of adsorption sites as a result of overcrowding results in deactivation of activated molecules by collision with ground state molecules dominates the reaction and also increase in turbidity of the solution reduces the light transmission through the solution, thus reducing the rate of reaction initiate the degradation reaction [30-33]. So, the photodegradation was most effective at 97.35% 0.3g/100ml for $NiCaO_2$-I and 95.03% 0.4g/100ml for $NiCaO_2$-II nano-particle dosages, further experiments were continued with same dosages.

3.8. EFFECT OF PH

The effect of pH on the degradation of CBBG dye was investigated varying pH ranging from 2 to11.The results illustrated that, the degradation efficiency affected by pH. The percentage of degradation on CBBG dye for $NiCaO_2$-I (Figure 4c) (Figure 5c) increased from 85.54% to 98.12% from pH 2 to pH 6 and decreased to 81.34% at pH 11 in 120 minutes for 0.3g/100ml. For $NiCaO_2$-II (Figure 4d) (Figure 5d) the degradation of the CBBG increased from 84.43% to 96.90% from pH 2 to pH 3 and decreased 78.14% at pH 11 in 120 minutes for 0.4g/100ml. The maximum percentage of degradation for the two different nanoparticles was achieved at pH 6 in $NiCaO_2$-I and pH 3 in $NiCaO_2$-II.

The effect of pH explained on the basis of zero point charge (ZPC) of $NiCaO_2$-I and $NiCaO_2$-II nanoparticles, where zero point charge of $NiCaO_2$-I and $NiCaO_2$-II was 11.5 and 11.7 respectively shown in Figure 3a. $NiCaO_2$-I and $NiCaO_2$-II nanoparticles surface is positively charged with below the 11.5 and 11.7pH. The CBBG is an anionic dye, the surface were attracted more towards the surface of catalyst and excess of hydroxyl anions increases the formation of $OH^{\bullet}$ radicals. These OH^- ions will generate more $^{\bullet}OH$ radicals by combining with the hole of the semiconductor and the $OH^{\bullet}$ radicals are the main oxidizing species responsible for photocatalytic degradation. On higher pH the decrease in degradation capacity can be explained on the basis of the amphoteric nature of the catalysts. Here the catalyst surface becomes negatively charged for higher pH value, which causes the electrostatic repulsion between the catalyst and negatively charged dyes [14, 34-38].

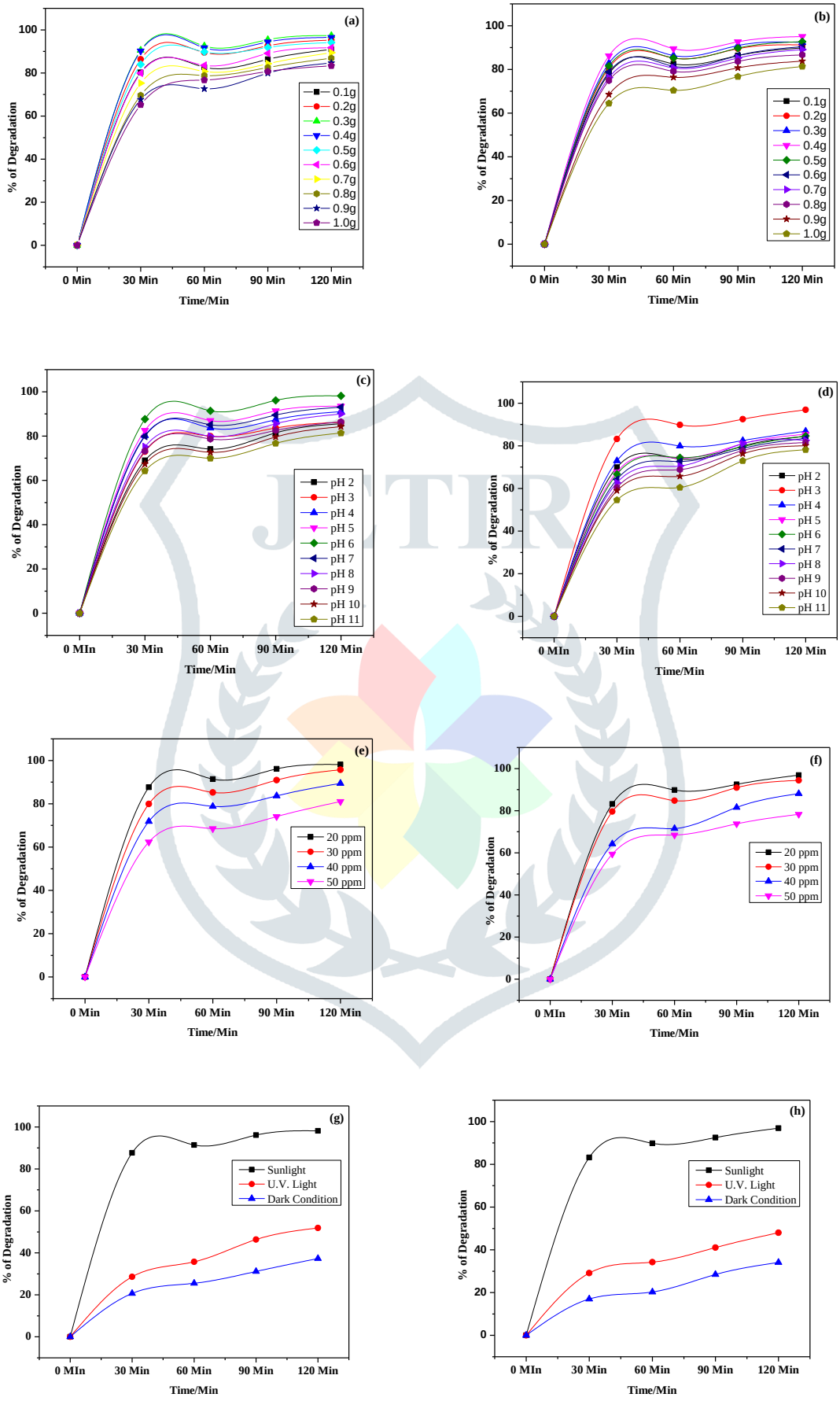

Figure 4: Degradation of Dye with respect to time, Catalyst Concentration (a) $NiCaO_2$-I (b) $NiCaO_2$-II, effect of pH (c) $NiCaO_2$-I (d) $NiCaO_2$-II, dye concentration (e) $NiCaO_2$-I (f) $NiCaO_2$-II, effect of sunlight irradiation (g) $NiCaO_2$-I (h) $NiCaO_2$-II,

3.9. EFFECT OF INITIAL DYE CONCENTRATION

The experiments were conducted to study the effect of initial dye concentration by varying the CBBG dye concentration from 20 ppm to 50 ppm. The results obtained for $NiCaO_2$-I (Figure 4e) (Figure 5e) is 98.12% for 20ppm, 96.69% for 30ppm, 89.40% for 40ppm and 81.01% for 50ppm. And for $NiCaO_2$-II (Figure 4f) (Figure 5f) is 96.90% for 20ppm, 94.37% for 30ppm, 88.07 for 40ppm and 78.25% for 50ppm, these experiments illustrated that the degradation efficiency was directly affected by the concentration. When the dye concentration increases, the amount of dye adsorbed or radiation photons to the catalytic surface increases and the photons get intercepted before they can reach the catalyst surface is blocked and separated, decreasing the absorption of photons by the catalyst [39] and the equilibrium adsorption of dye on the catalyst surface which results in a decrease in the active sites. This phenomenon results in the lower formation of $OH^{\bullet}$ radicals which were considered as primary oxidizing agents of the organic dye [19]. As per the Beer Lambert law, if the primary dye concentration increases, the photons entering the dye solution decreases. These activities results in the decreased photocatalytic reaction rate as there will be lower photon adsorption for the catalyst particles [20].

3.10. EFFECT OF SUNLIGHT IRRADIATION

The photocatalytic degradation of CBBG dye (20mg/L) under three different experimental conditions were examined, *i.e.*, through sunlight alone, dye/dark/catalyst, dye/UV/catalyst and dye/sunlight/catalyst for the catalyst. CBBG dye solution when exposed directly to the sunlight without the catalyst, the degradation was found to be nil during the entire experiments. The degradation rate was found to increase with increase in irradiation time, for dye/sunlight/ $NiCaO_2$-I showed 98.12%, dye/UV/ $NiCaO_2$-I found to be 51.87% and for dye/dark/ $NiCaO_2$-I 37.30% was recorded (Figure 4g) (Figure 5g).Similarly for CBBG dye (20mg/L) for dye/sunlight/ $NiCaO_2$-II showed 96.90%, dye/UV/ $NiCaO_2$-II found to be 48.01% and for dye/dark/ $NiCaO_2$-II 34.10% was recorded (Figure 4h) (Figure 5h).These results clearly indicate that, photodegradation occurs most efficiently in the presence of sunlight. Under sunlight, excitation of electrons from the catalyst surface takes place more rapidly than in the absence of light. Similar reports have been reported for photocatalytic degradation of dyes. [21].

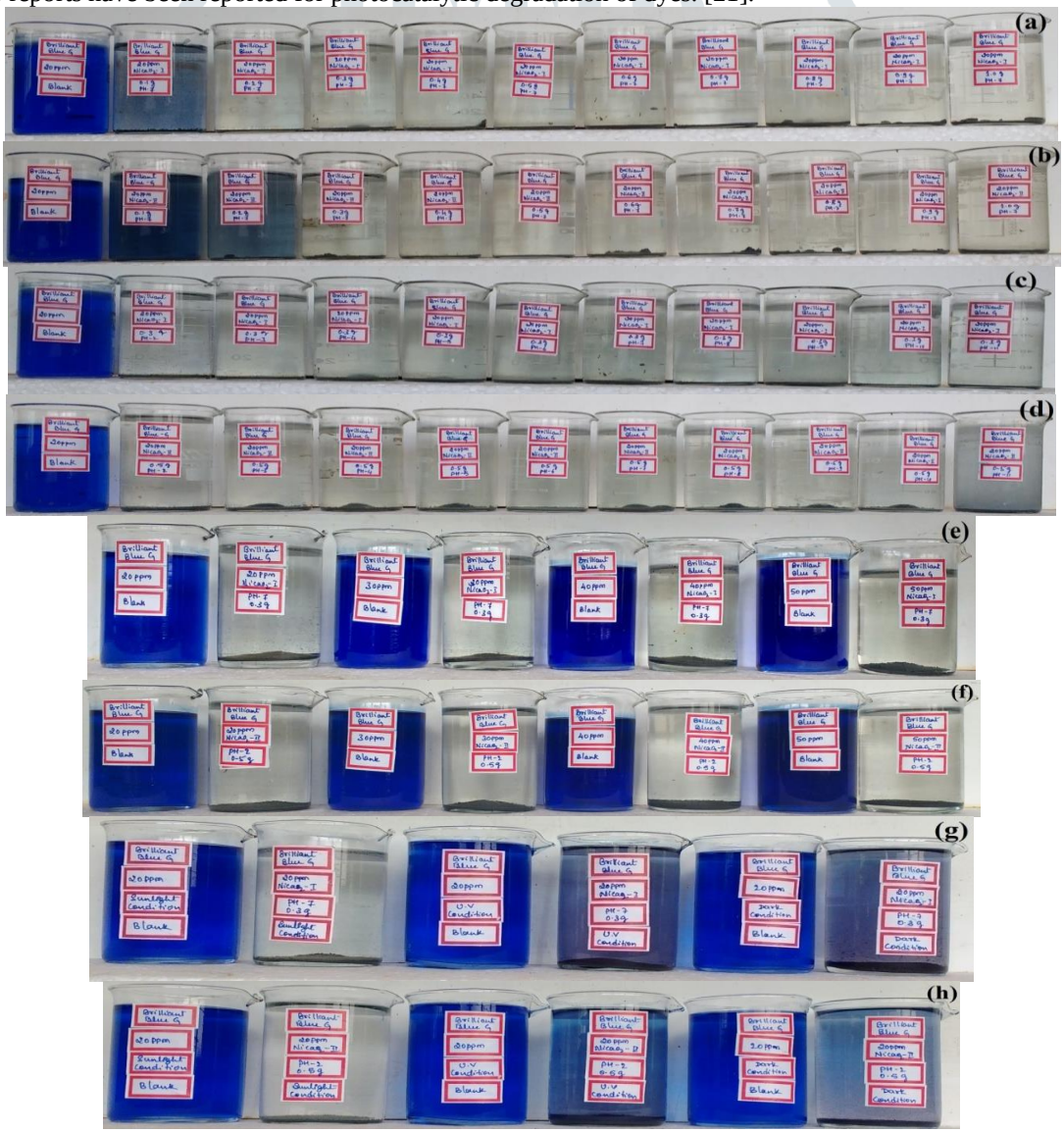

Figure 5: Degradation of CBBG dye**,** effect of catalyst concentration (a) $NiCaO_2$-I (b) $NiCaO_2$-II, effect of pH (c) $NiCaO_2$-I (d) $NiCaO_2$-II, effect of initial dye concentration (e) $NiCaO_2$-I (f) $NiCaO_2$-II, effect of sunlight irradiation with respect to dark and U.V. conditions (g) $NiCaO_2$-I (h) $NiCaO_2$-II.

3.11. REUSE OF CATALYST

The $NiCaO_2$-I and $NiCaO_2$-II nanoparticles were tested for reusability and the efficiencies of the $NiCaO_2$-I nanoparticle in the first and second reuse were 93% and 89% and for the $NiCaO_2$-II nanoparticle in the first and second reuse were 91% and 87% (Figure 6). The slight decrease of photocatalytic efficiency could be due to leaching of active sites on catalyst surface and loss of the catalyst during separation. Hence these nanoparticles were shown good results in the reuse and this can be applicable in the waste water treatment in industries [27].

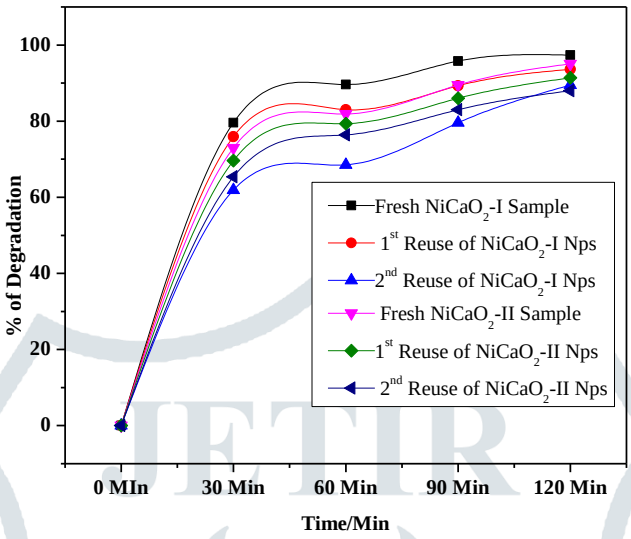

Figure 6: Reuse of Catalyst with respect to time

4. CONCLUSION

The present study reveals that, the Nickel Calciate nanoparticles decolourised CBBG more efficiently in a shorter interval of time in presence of sunlight as a source of irradiation. The proposed photocatalytic methods proved very effective as we have achieved 98.12% degradation in pH 6 and 98.01% degradation at pH 3 for $NiCaO_2$ nanoparticles for the small size of the $NiCaO_2$-I (14nm) and $NiCaO_2$-II (19nm).Hence, it can be concluded that the size of the nano materials play significant role for the degradation of dyes. And these results can help in the treatment of textile effluents which are causing pollution to the environment.

REFERENCE

[1]. Sangareswari. M., and Sundaram, M.M. (2015). Enhanced Photocatalytic Activity of Conducting Polypyrrole-TiO_2 Nanocomposite for Degradation of Organic Dyes under UV Light Irradiation, *Journal of Nanoscience and Technology*, 1(1): 9-12.

[2]. Giwa, A., Nkeonye, P.O, Bello, K.A, and Kolawole, E.G. (2015). Solar Photocatalytic Degradation of Reactive Yellow 81 and Reactive Violet 1 in Aqueous Solution Containing Semiconductor Oxides, *International Journal of Applied Science and Technology*, 2(4): 90-105.

[3]. Yogendra, K., Naik, S., Mahadevan, K.M., and Madhusudhana, N. (2011). A comparative study of photocatalytic activities of two different synthesized ZnO composites against Coralene Red F3BS dye in presence of natural solar light, *International Journal of Environmental Sciences and Research*, 1(1): 11-15.

[4]. Chatzisymeon, E., Petrou, C., and Mantzavinos, D. (2013). Photocatalytic treatment of textile dyehouse effluents with simulated and natural solar light, *Global Nest Journal*, 15(1): 21–28.

[5]. Akpan, U.G, and Hameed, B.H. (2009). Parameters affecting the photocatalytic degradation of dyes using TiO_2-based photocatalysts: A review, *Journal of Hazardous Materials*, 170(2-3): 520–529.

[6]. Parra, M.R., and Haque, F.Z. (2014). Aqueous chemical route synthesis and the effect of calcination temperature on the structural and optical properties of ZnO nanoparticles, *Journal of Material Research and Technology*, 3(4): 363-369.

[7]. Rauf, M.A., Ashraf, S., and Alhadrami, S.N. (2005). Photolytic oxidation of Coomassie Brilliant Blue with H_2O_2, *Dyes and Pigments*, 66: 197-200. doi:10.1016/j.dyepig.2004.09.006.

[8]. Raza, W., Haque, M.M., Muneer, M., Harada, T., and Matsumura, M. (2015). Synthesis, characterization and photocatalytic performance of visible light induced bismuth oxide nanoparticle, *Journal of Alloys and Compounds*, 648: 641–650. DOI 10.1016/j.jallcom.2015.06.245.

[9]. Haque, M.M., Raza, W., Muneer, M., Fleisch, M., Hakki, A. and Bahnemann, D. (2015). Photocatalytic degradation of different chromophoric dyes in aqueous phase using La and Mo doped TiO_2 hybrid carbon spheres, *Journal of Alloys and Compounds*, 632; 837–844. doi.org/10.1016/j.jallcom.2015.01.222.

[10]. Papnai, N., and Ameta, K.L. (2014). Cerium-Iron Oxide Catalyzed Photodegradation of Brilliant Blue G, *Chemical Science Transactions*, 3(3): 1001-1006. DOI:10.7598/cst2014.841

[11]. Kora, A.J., and Rastogi, L. (2016). Catalytic degradation of anthropogenic dye pollutants using palladium nanoparticles synthesized by gum olibanum, a glucuronoarabinogalactan biopolymer, *Industrial Crops and Products*, 81: 1–10.

[12]. Jadhav, S.U., Jadhav, M.U., Kagalkar, A.N., and Govindwar, S.P. (2008). Decolorization of Brilliant Blue G dye mediated by degradation of the microbial consortium of Galactomycesgeotrichum and *Bacillus sp*. *Journal of the Chinese Institute of Chemical Engineers*, 39: 563–570. doi:10.1016/j.jcice.2008.06.003

[13]. Arunachalam, R., Dhanasingh, S., Kalimuthu, B., Uthirappan, M., Rose, C. and Mandal, A.B. (2012). Phytosynthesis of silver nanoparticles using Cocciniagrandis leaf extract and its application in the photocatalytic degradation, *Colloids and Surfaces B: Biointerfaces*, 94: 226– 230. doi:10.1016/j.colsurfb.2012.01.040

[14]. Gopalappa, H., Yogendra, K., Mahadevan, K.M., and Madhusudhana, N. (2014). Solar Photocatalytic Degradation of Azo Dye Brilliant Red in Aqueous Medium by Synthesized $CaMgO_2$ Nanoparticle as an Alternative Catalyst, *Chemical Science Transactions*, DOI:10.7598/cst2014.708.

[15]. Bhavya, C., Yogendra, K., and Mahadevan, K.M. (2015). Synthesis of Calcium Aluminate Nanoparticle and Its Application to Photocatalytic Degradation of Coralene Navy Blue 3G and Coralene Violet 3R, *International Journal of Research in Chemistry and Environment*, 5(1): 28-33.

[16]. Lodha, S., Jain, A., and Punjabi, P.B. (2011). A novel route for waste water treatment: Photocatalytic degradation of Rhodamine B, *Arabian Journal of Chemistry*, 4(4): 383–387.

[17]. Uddin, M.J., Islam, M.A., Haque, S.A., Hasan, S., Amin, M.S.A., and Rahman, M.M. (2012). Preparation of nanostructured TiO2-based photocatalyst by controlling the calcining temperature and pH, *International Nano Letters*, 2(1): 1-10.

[18]. Bhavya, C., Yogendra, K., and Mahadevan, K.M. (2015). A Study on the Synthesis, Characterization and Photocatalytic Activity of CaO Nanoparticle against Some Selected Azo Dyes, *Indian Journal of Applied Research*, 5(6): 361–365.

[19]. Gopalappa, H., Yogendra, K., Mahadevan, K.M., and Madhusudhana, N. (2012). A comparative study on the solar photocatalytic degradation of Brilliant Red azo dye by CaO and $CaMgO_2$ nanoparticles, *International Journal of Science Researc*h, 1(2): 91–95.

[20]. Madhusudhana, N., Yogendra, K., and Mahadevan, K.M. (2012). A comparative study on Photocatalytic degradation of Violet GL2B azo dye using CaO and TiO_2 nanoparticles, *International Journal of Engineering Research and Applications* (IJERA), 2(5): 1300-1307.

[21]. Madhusudhana, N., Yogendra, K., and Mahadevan, K.M. (2013). photocatalytic decolourization of textile effluent by using metal oxide nanoparticles, *Journal of Science and Arts*, 3(24): 303-318.

[22]. Madhusudhana, N., Yogendra, K., and Mahadevan, K.M. (2014). Photocatalytic decolourization of Textile Effluent by using Synthesized Nano particles, *Journal of Environmental. Nanotechnology*, 3(4): 41-53.

[23]. Ge, M., Zhu, N., Zhao, Y., Li, J., and Liu, L. (2012). Sunlight-Assisted Degradation of Dye Pollutants in Ag_3PO_4 Suspension, *Industrial and Engineering Chemistry research*, 51: 5167−5173

[24]. Meng, X., Zhang, L., Dai, H., Zhao, Z., Zhang, R., and Liu, Y. (2011). Surfactant-assisted hydrothermal fabrication and visible-light-driven photocatalytic degradation of methylene blue over multiple morphological $BiVO_4$ single-crystallites, *Materials Chemistry and Physics*, 125: 59–65.

[25]. Ghorai, T.K., and Biswas, N. (2013). Photodegradation of rhodamine 6G in aqueous solution via $SrCrO_4$ and TiO_2 nano-sphere mixed oxides, *Journal of Materials Science and Technology*, 2(1): 10-17.

[26]. Patil, B.N., and Naik, D.B., and Shrivastava, V.S. (2010). Photocatalytic degradation of hazardous Ponceau-S dye from industrial wastewater using nanosized niobium pentoxide with carbon, *Desalination*, 269: 276–283.

[27]. Kulkarni, S.D., Kumbar, S., Menon, S.G., Choudhari, K.S., and Santhosh, C. (2016). Magnetically separable core–shell $ZnFe_2O_4$@ZnO nanoparticles for visible light photodegradation of methyl orange, *Materials Research Bulletin*, 77: 70–77.

[28]. Santhosh, A.M., Yogendra, K., Mahadevan, K.M., and Madhusudhana, N. (2018). Application of Nickel Calciate Nanoparticles in the Photodegradation of direct green 6 dye, *International Research Journal of Environmental Sciences*, 7(6): 12-18.

[29]. Parthibana, C., and Sundaramurthy, N. (2015). Biosynthesis , Characterization of ZnO Nanoparticles by Using PyrusPyrifolia Leaf Extract and Their Photocatalytic Activity, International, *Journal of Innovative Research in Science, Engineering and Technology*, 4(10): 9710-9718.

[30]. Byrappa, K., Subramani, A.K., Ananda, S., Lokanatha-Rai, K.M., Dinesh, R., and Yoshimura, M. (2006). Photocatalytic degradation of Rhodamine B dye using hydrothermally synthesized ZnO, *Bulletin of Material Sciences*, 29**:** 433-438.

[31]. Habib, A., Muslim, M., Shahadat, M.T., Islam, M.N., Mohmmad, I., & Ismail, I.M.I., Islam, T.S.A. and Mahmood, A.J. (2013). Photocatalytic decolourization of crystal violet in aqueous nano-ZnO suspension under visible light irradiation, *International Nano Letters*, 3(5): 1-8.

[32]. Sakthivel, S., Neppolian, B., Shankar, M.V.,Arabindoo, B., Palanichamy, M. and Murugesan, V. (2003). Solar Photocatalytic Degradation of Azo Dye : Comparison of Photocatalytic Efficiency of ZnO and TiO_2, *Solar Energy Materials & Solar Cells*, 77: 65–82.

[33]. Subramani, A.K., Byrappa, K., Ananda, S., Lokanatha Rai, K.M., Ranganathaiah, C. and Yoshimura, M. (2007). Photocatalytic degradation of indigo carmine dye using TiO_2 impregnated activated carbon, *Bulletin of materials science*, 30**:** 37-41.

[34]. Guillard, C., Lachheb, H., Houas, A., Ksibi, M., Elaloui, E., and Herrmann, J. M. (2003). Influence of chemical structure of dyes, of pH and of inorganic salts on their photocatalytic degradation by TiO_2 comparison of the efficiency of powder and supported TiO_2, *Journal of Photochemistry and Photobiology A: Chemistry*, 158: 27–36.

[35]. Mehta, R., and Surana, M. (2012). Comparative study of photo-degradation of dye Acid Orange -8 by Fenton reagent and Titanium Oxide- A review, *Der Pharma Chemica*, 4(1): 311-319.

[36]. Mehta, P., Mehta, R., Surana, M., and Kabra, B.V. (2011). Influence of Operational Parameters on Degradation of Commercial Textile Azo Dye Acid Blue 113 (cyanine 5R) by Advanced Oxidation Technology, *Journal of Current Chemical and Pharmaceuticals Sciences*, 1(1): 28-36.
[37]. Sangari, N.U., and Velusamy, P. (2016). Photocatalytic Decoloration Efficiencies of ZnO and TiO_2 : A Comparative Study, *Journal of Environmental Science and Pollution Research*, 2(1): 42–45.
[38]. Turchi, C.S., and Ollis, D.F. (1990). Photocatalytic Degradation of Organic Water Contaminants: Mechanisms Involving Hydroxyl Radical Attack, *Journal of Catalysis*, 122: 178-192.
[39]. Chakrabarti, S., and Dutta, B.K. (2004). Photocatalytic degradation of model textile dyes in wastewater using ZnO as semiconductor catalyst, *Journal of Hazardous Material B*, 112: 269–278.